Morphological Aspects of Ciliary Motility

PETER SATIR

From the Department of Zoology, University of Chicago

ABSTRACT In *Elliptio complanatus* lateral cilia, two distinct patterns of filament termination can be discerned. In one case, all nine filaments are present and all are single; in the second, at least one filament is missing but doublets are still present. These probably represent different configurations within one cilium in different stroke positions; to get from one to the other, some peripheral filaments must move with respect to others. The data are consistent with the hypothesis that the filaments themselves do not change length, but rather slide past one another to accommodate increasing curvature. The bent regions of the cilium are in the form of circular arcs. In a few cases, apparent displacement of filaments at the tip (Δl) can be shown to be accounted for if we assume that all differences are generated within these arcs. The displacement per degree of bend is 35 A. Regions of bent arc are initially confined to the base of the cilium but move up the shaft as straight regions appear below them. From the relationship between arc length and radius of curvature, a shaft length that is the unit that initially bends and slides may be defined. Quantal displacements of the length of one 14S dynein may perhaps occur at sites between filaments at opposite sides of such a unit as sliding occurs.

The cilium is a motile, long, flexible, thin, membrane-bound cylinder that tapers slightly to a blunt point at its distal end and projects from the apical ends of many cells. The length of the cylinder varies but is usually about 5–15 μ, or roughly 25–75 times its width. Operationally, the cilium is best defined morphologically, by its electron microscope cross-section: the 9 + 2 pattern. There is no detectable difference in axonemal structure between cilia and many eucaryotic flagella, although sperm tails in general show somewhat greater variation. The length and arrangement of flagella on the cell may be different from cilia; the beat pattern is different, but the axonemal arrangement and diameter are usually constant (1–3).

Within the axoneme lies the mechanism of motion. Cilia may be isolated from cells, or their membrane coating may be stripped away while much of the axoneme stays in place. Such naked axonemes retain the ability to move under proper ionic conditions upon addition of ATP (2, 4). Fractions have been prepared of the membrane and of filament-associated proteins of cilia. In particular, Gibbons (5) has demonstrated at ATPase—dynein—that is

associated with the axoneme and specifically with the arms that are regularly spaced some 170–200 A (6, 7) (175 A in *Elliptio*) apart on the nine peripheral filaments. Dynein can be prepared as a 30S protein fraction which is a polymer of 14S subunits. In shadowed preparations, 30S dynein is a rod-like molecule with an average length of 1700 A (8), composed of particles 140 A long. The latter presumably correspond to the arms (the differences in dimension are accounted for by the varying techniques).

The problem of correlation of structure and function in ciliary motility lends itself to the potentialities of the electron microscope in the area of quick fixation, where rather fast processes requiring only a few milliseconds for completion may be dissected. With a quick fixation method we may hope to freeze the morphological, perhaps even the molecular, indicators of the axonemal changes accompanying, or producing, motion. The following is an account of our present progress.

FIXATION OF THE METACHRONAL WAVE

The idea of quick fixation of cilia is not a very new one; in 1927, Gelei applied such a technique in preserving the appearance of the metachronal wave of *Paramecium*. When there is a beat phase difference between neighbors in a field of cilia, wave fronts appear. One wavelength contains cilia in one beat cycle (9). Preservation of the form of the waves captures the individual cilia in separate phases of beat (10).

For electron microscope study of the morphology of the components of a fixed metachronal wave, *Paramecium* is too sparsely ciliated an organism except in the oral region. A better material is the lateral cells of the gills of lamellibranch molluscs. In the fresh water mussel *Elliptio*, there are four rows of such cells on each side of a gill filament. Each cell contains four or five rows of approximately 50 cilia, each 14 μ long, which are spaced at intervals of about 0.35 μ. Between the cilia there are short (1 μ long) microvilli. Under appropriate conditions, the cilia beat with a frequency of about 17 beats/sec (1 beat every 59 msec) (11), and a metachronal wavelength of about 11.4 μ or 31 cilia (some 20 of these are in the recovery stroke, and the phase difference between them is just about 1.9 msec) (Table I). The rate of penetration of osmium tetroxide through tissue is slow, but the radius of the exposed ciliary shaft is only some 125 mμ. It seems likely that even the phase difference between single cilia could be preserved in the fixation procedure.

The best measurements of the slope of the fixed wave so far show a progression of about 0.5 μ between cilia [see Fig. 12 of Satir (10)]. This is about three-quarters of the expected value. Thus, we can detect differences between adjacent cilia. There seems, then, no doubt that the grosser, as well as many finer, aspects of beat form are captured in the micrographs, although the fastest molecular processes may not be effectively preserved.

FORM OF THE BEAT

Single stroke stages may be studied. Interestingly, the stroke form can be constructed from circular arcs and tangential straight regions for all stages examined. Brokaw (4, 12) and Brokaw and Wright (13) have recently shown a similar situation for spermatozoa.

From electron micrographs (Figs. 1–3) a relation between arc length (A) of the bent region of the cilium (measured at the center of the axoneme) and

TABLE I

MORPHOLOGY OF THE FIXED METACHRONAL WAVE

	λ	Cilia/λ	Effective stroke	Recovery stroke
	μ			
	9.4			
	9.	34	12	22
	11.	30	13	17
	11.8	29	10	19
	15.	33	11	22
	12.5	30	10	20
Average	11.4	31.2	11.2	20.0
msec	(59)		(21)	(38)
Movie reconstruction			13.4	17.8
Satir (11)			(25)	(34)
Stroke reconstruction			14.3	16.9
Table II			(27)	(32)

angle (α) can be determined, where

$$\frac{A}{\alpha} = \frac{2\pi r}{360} \qquad (1)$$

r being the radius of curvature of the arc (α and r can be measured independently). The plot of A vs. α is not linear (that is, r is not a constant), but rather an empirical fit is obtained for the parabola (Fig. 4)

$$(\alpha - 35)^2 = 920\,(A - 1.5) \qquad (2)$$

where α is measured in degrees and A in microns. The equation applies to all bent arcs irrespective of length or stroke stage, provided that the leading edge of the arc has not reached the tip of the cilium. Apparently, Brokaw's (12) data are accommodated as well.

Regions of bend are initiated at the base of the cilium, grow to a certain arc length, and then move up the ciliary shaft as straight regions appear below them (Fig. 5). During the last process, α changes little if at all, and the radius of curvature of the arc is constant. For *Elliptio* lateral cilia, the highest angular

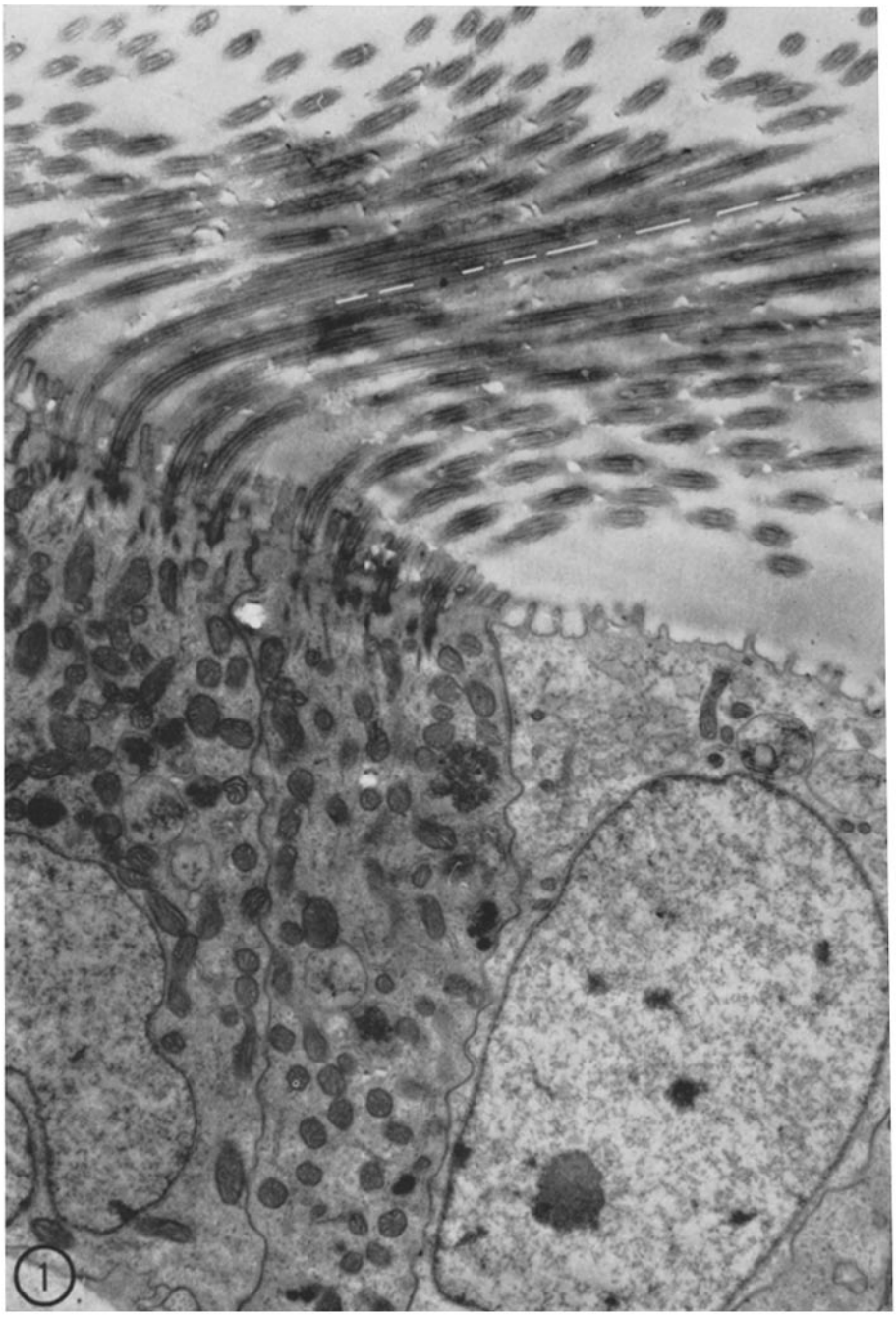

FIGURE 1

bends measure about 97° in an abfrontal direction. In the frontal direction the bends appear to be slightly less, about 81°. The straight portions separating the bends are also quite different in length, the longer region occurring after the longer arc. By this process an asymmetrical beat is generated, which, coupled with the short length of the cilium, produces the characteristic flexural motion (Figs. 6–8). In contrast, the symmetrical arcs and corresponding straight regions of flagella, coupled with the longer length, yield undulatory motion. It is convenient to label the arcs and straight portions A_1–A_4, where A_1 is the shortest straight region and A_2 and A_4 are arcs in the abfrontal and frontal directions, respectively. The generation of straight region A_1 and arc A_2 accounts for the effective stroke of the cilium (Fig. 8), while the generation of A_3 and A_4 accounts for the recovery stroke (Fig. 7). The rate of movement (v_s) along the shaft is a constant to a first approximation and

$$A_x = v_s t_x \tag{3}$$

where t_x is the time corresponding to the generation of region A_x. Regions A_1–A_4 are generated during one beat and, accordingly, $v_s \sim 3.5 \times 10^2\ \mu$/sec (Table II). Regions A_1 and A_2 are generated in approximately 27 msec; A_3 and A_4 in 32 msec, in reasonable agreement with the effective vs. recovery stroke times as measured by other means (Table I).

ROLE OF THE PERIPHERAL FILAMENTS

One piece of direct evidence can be presented to implicate the peripheral filaments in the bending process. At the tapering end of the cilium, the peripheral filament structure simplifies to a single microtubule prior to termination. In doing so, first the arms and then subfiber *b* of each doublet disappear. Two patterns have been discerned in these tips, sometimes as close as six cilia apart within one fixed wavelength. The patterns cannot be derived from one another; each is so frequently observed that it is difficult to consider it simply a developmental variant. In one case, all nine peripheral filaments are present and all are single; in the second, at least one filament is missing but doublets are still present (Figs. 9 and 10). If these really represent differing configurations within one cilium at different times, to get from one to the other some peripheral filaments must move with respect to others. A number of hypotheses

---

FIGURES 1–3. Electron micrographs illustrating stroke form and measurement of A, α, and r [similar micrographs also appear in Figs. 31–34 of Satir (11) and Fig. 28 of Satir (14)].

FIGURE 1. Frontally pointing cilia. Dashed white line illustrates part of the straight portion (A_3) of one cilium measured along the central pair. Arc length (A_4) and α_4 may be measured at bases of adjacent cilia if similar straight portions are extended back to the point where they are tangent to the arc. × 10,500.

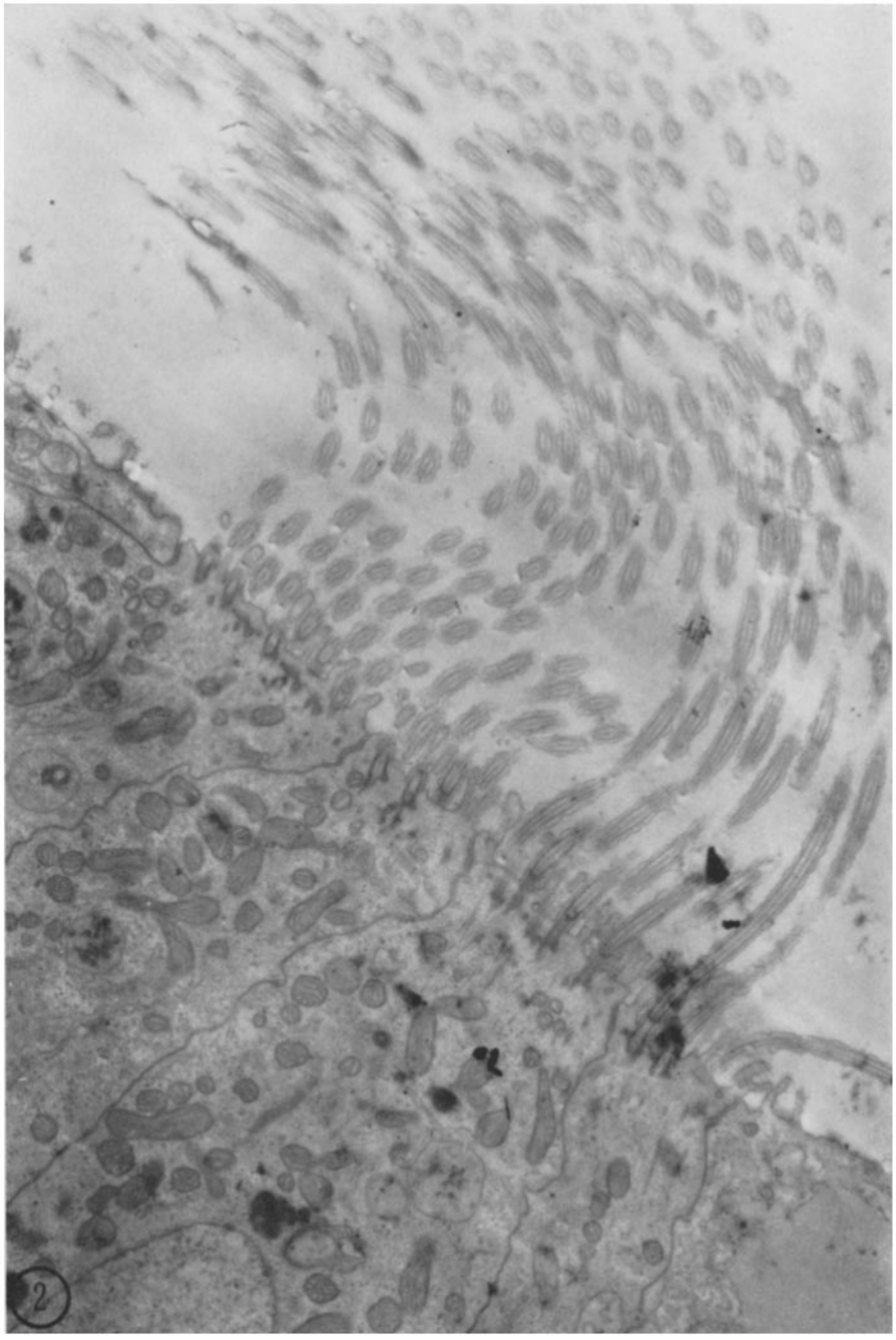

FIGURE 2

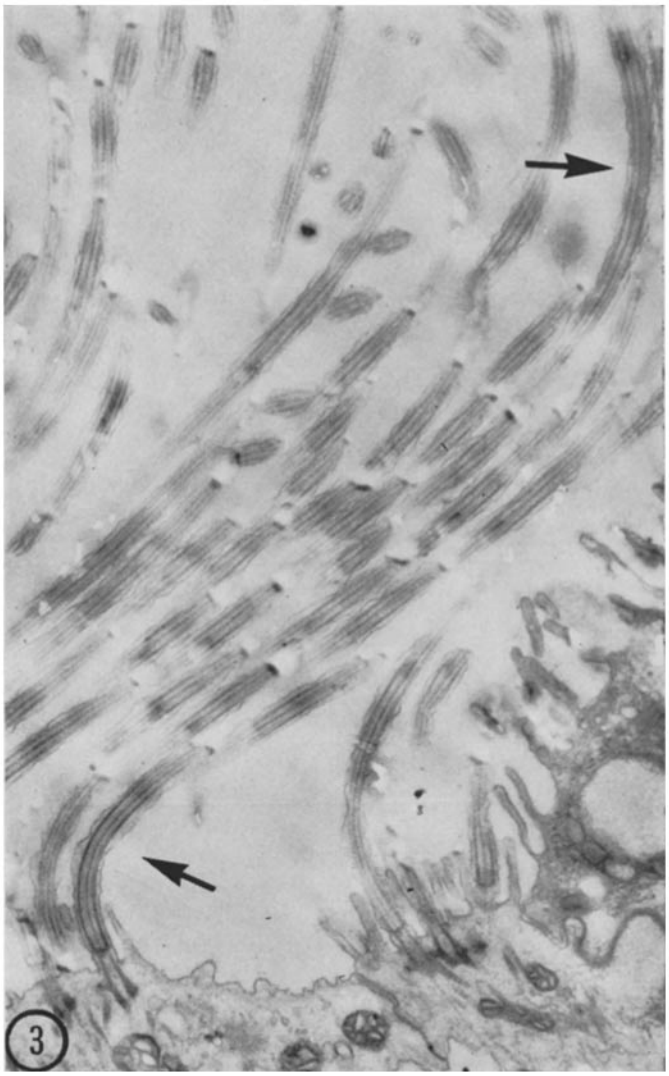

FIGURE 3. S-shaped cilia, probably in late recovery stroke. Note that radius of curvature of arc (A_4) at base is less than radius of curvature of arc (A_2) farther along shaft (arrows). The two curves are separated by straight region A_3. × 21,000.

of ciliary motility that would account for such relative motion have been considered in the past, of which the most highly regarded at present are either that the filaments themselves contract (shorten) to bend the cilium, or that the filaments do not change length during the beat but are displaced (slide) to

FIGURE 2. Abfrontally pointing cilia. Oblique section. Note that straight portion (A_3) of cilium is adjacent to basal body in this micrograph. Curved region length and radius of curvature may be estimated by connecting portions of successive cilia. × 10,500.

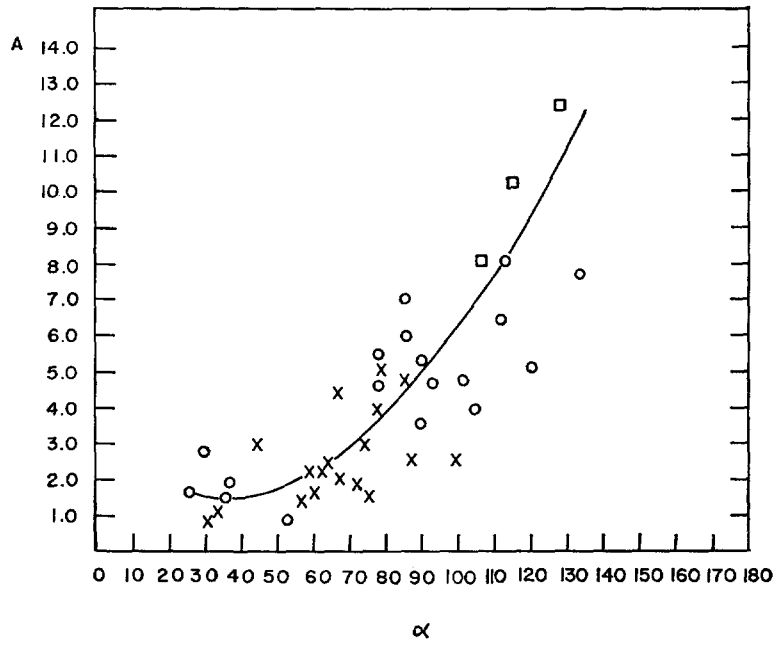

FIGURE 4. Relationship of arc length (A), in microns, and angle (α), in degrees, subtended by the arc. ○, abfrontal arcs (A_2); ×, frontal arcs (A_4); □, data from Brokaw (12) on invertebrate sperm. The line plots equation 2.

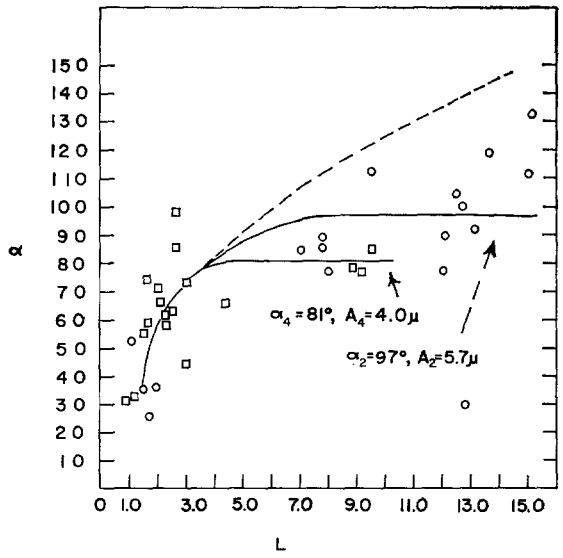

FIGURE 5. Relationship of α to distance (L) between front of the bent arc and the ciliary basal body. Dashed line plots equation 2 if L is equal to A. ○, abfrontal arcs (A_2); □, frontal arcs (A_4). The low point at $L = 12.8\mu$ probably represents an arc that has reached the cilium tip.

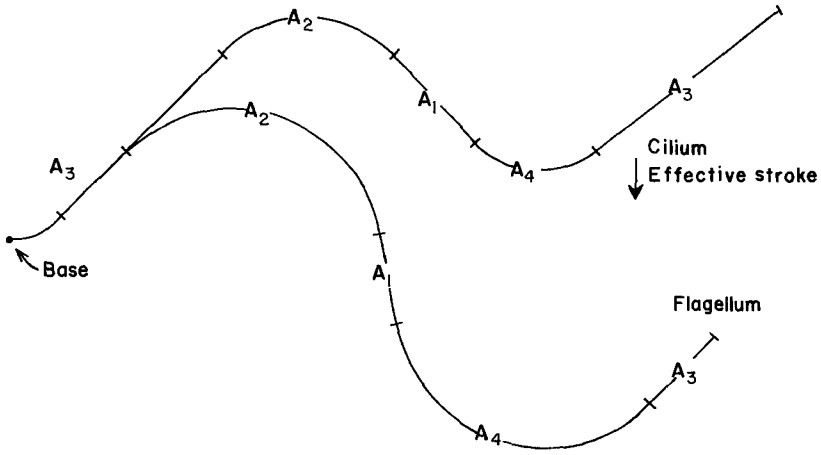

FIGURE 6. Flexural vs. undulatory motion. In flagella, when region $A_1 = A_3$ and $A_2 = A_4$, the wave is symmetrical. Coupled with the relatively long length of the organelle, this symmetry gives undulatory motion. In cilia, where $A_3 > A_1$ and $A_2 > A_4$, the unequal bending, coupled with the relatively short length, gives an effective and recovery stroke, and flexural motion.

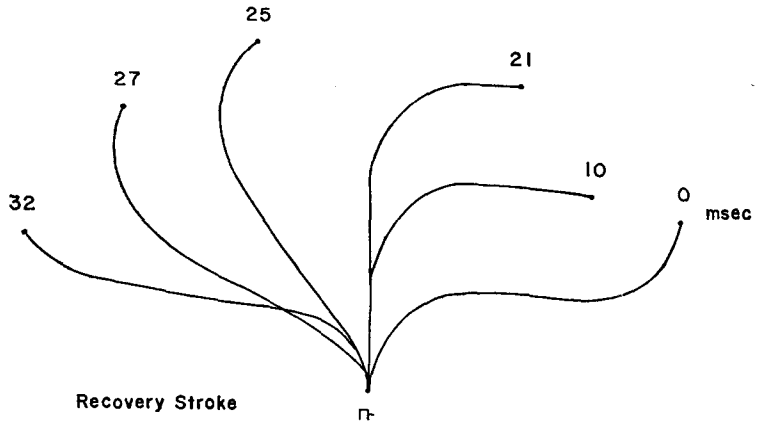

FIGURES 7–8. Constructed beat forms for a typical lateral cilium of *Elliptio*.
FIGURE 7. Recovery stroke, occupying the first 32 msec of the beat, generated as straight region A_3 and arc A_4 appear at base of cilium. At 10 msec, stroke form corresponds to that seen in Fig. 2; at 27 msec, to Fig. 3; at 32 msec, to Fig. 1.

accommodate the increasing curvature. Further consideration of tip configuration and ciliary position allows a choice to be made between these alternatives.

TIP CONFIGURATION

A number of intermediate stages are usually present between the normal shaft 9 + 2 pattern and either one of the distinctive tip patterns. In these, the

singlets are not randomly interspersed among doublets but are grouped so that they are nearly always contiguous (this is not always true for flagella). Moreover, in a number of cases the singlets are distal to the cell surface over which the cilium is bent compared to the doublets. This is true for trematode (Jamuar, M. Personal communication) and frog pharyngeal, as well as for several types of *Elliptio* gill cilia (14). Cross-sections of this type are consistent

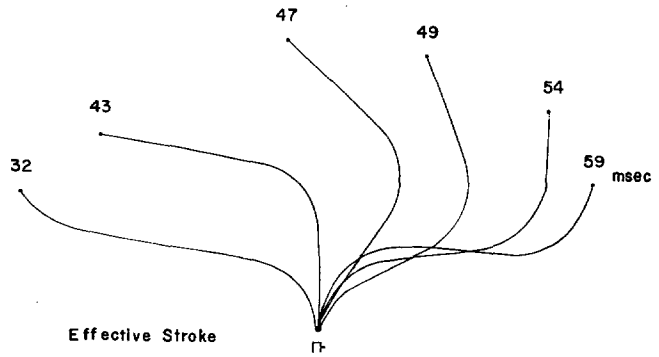

FIGURE 8. Effective stroke, occupying the last 27 msec of the beat, generated as straight region A_1 and arc A_2 appear at base of cilium.

TABLE II
STROKE PARAMETERS OF *ELLIPTIO* LATERAL CILIUM

Parameter	Value determined*	Number of measurements
A_1	3.7±0.4	4
A_2	5.7±0.9	11
A_3	7.1±0.4	7
A_4	4.0±0.7	3
A	20.5	
f	17±3‡	
v_s	349 μ/sec	

* Measurements are in microns, given with average error.
‡ Frequency from Satir (11).

with a model whereby the shorter-appearing filaments traverse the greater arc length, i.e. where all peripheral filaments are of equal length and the bottom filaments slide out as the cilium bends.

This conclusion can be made firmer in the case of the lateral cilia, where the wave may be fixed. Here, cilia may be found that bend in both directions, over the lateral and postlateral epithelium for the recovery stroke stages (Fig. 2), and back over the intermediate cell, toward the laterofrontal cirrus at the beginning of the effective stroke (Fig. 1). Accordingly, if a sliding model of

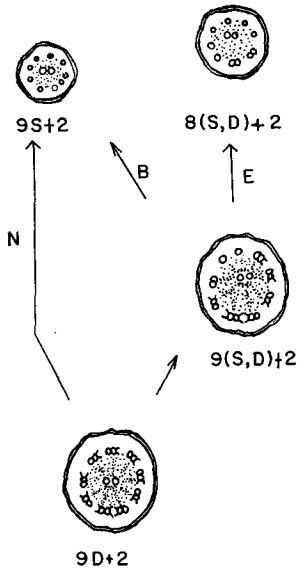

FIGURE 9. Possible methods of termination of the ciliary shaft. Peripheral doublets of normal shaft pattern (9D + 2) all end at one level in neutral (N-type) tips or they go through an intermediate mixed singlet-doublet pattern [9(S,D) + 2] before ending. Distal to 9(S,D) + 2 pattern, either a pattern with nine singlets (9S + 2) or eight or fewer filaments, some of which are doublets [8(S,D) + 2], can appear. The former (B-type tips) can be thought of as an intermediate between the neutral and extreme (E) types of tips.

filament action is correct, in both cases the filaments at the bottom of the ciliary cross-section should appear double but they should not be the same filaments. This may be shown to be the case (14).

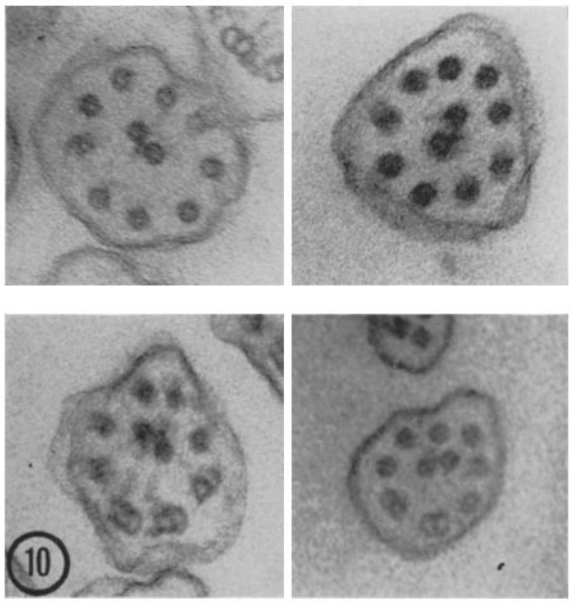

FIGURE 10. Illustrations of 9S + 2 vs. 8 (S,D) + 2 type tips. × 70,000 (top left and right); × 105,000 (bottom left); × 113,000 (bottom right).

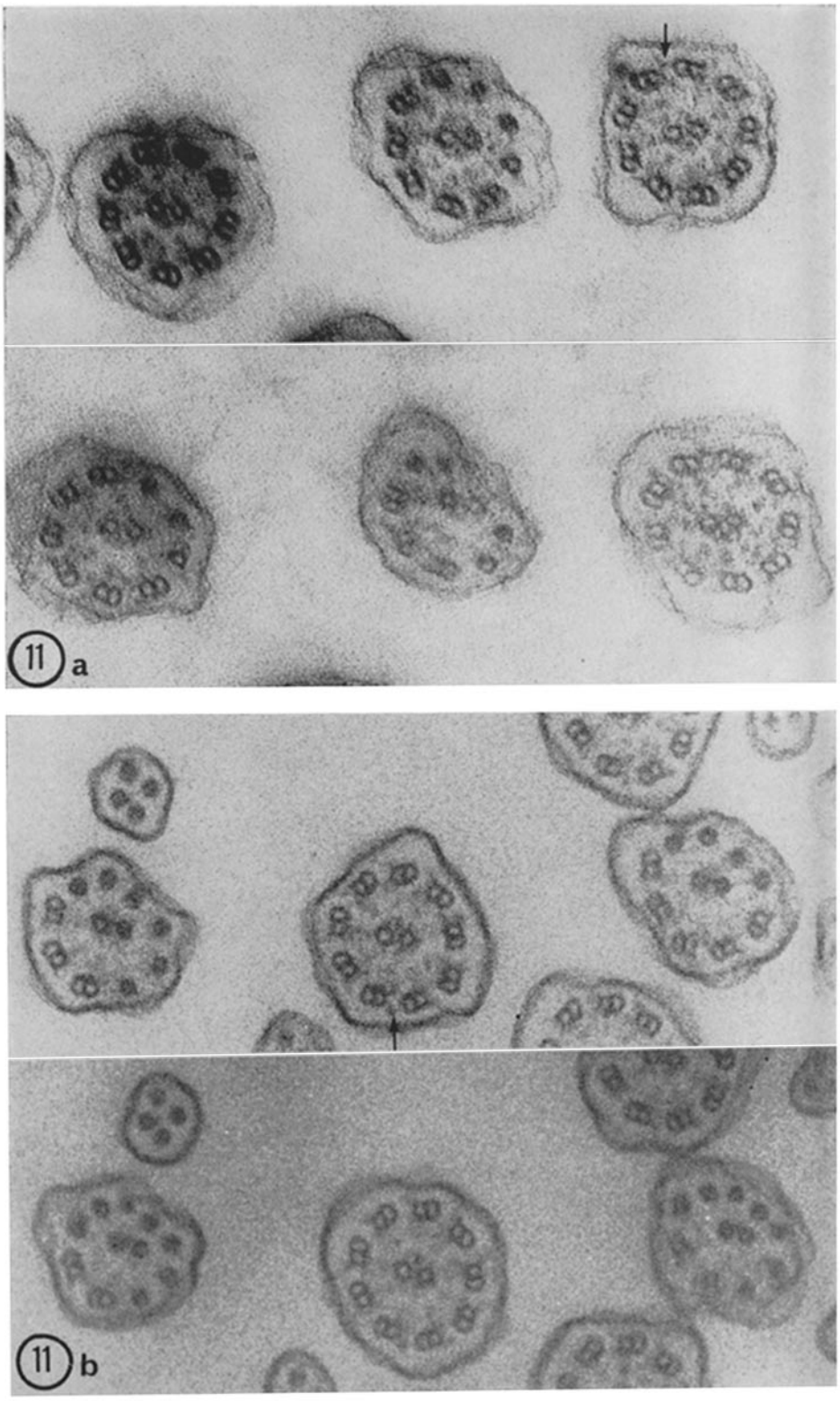

FIGURE 11

Filaments may be numbered with relative ease in cross-sections of mussel gill cilia. The distinctive bridge between filaments 5 and 6 is one characteristic marker. The edge of the cilium bearing filaments 5 and 6 is the leading edge during the effective stroke, and the trailing edge during recovery. In the former case, 5 and 6 are among the shorter-appearing filaments; in the latter, they are among the longer-appearing (Fig. 11). The exact order in which the filaments appear to terminate in any stroke stage is probably a reflection of the three-dimensional path of each filament at that moment. The torques

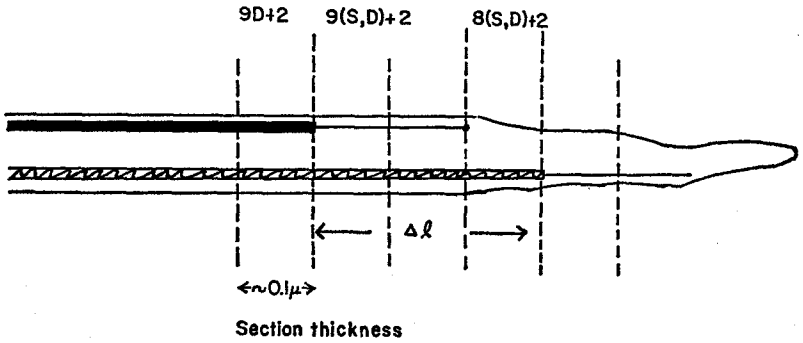

FIGURE 12. Calculation of Δl from serial sections (see Fig. 11*a*).

during the beat appear to be considerable enough to twist the shaft roughly 90° in 14 μ (6°/μ) to account for the systematic tilt of axis in cross-sections through fixed metachronal waves (10).

In a few cases, with the help of serial cross-sections, it is possible to estimate the distance between the longest- and shortest-appearing doublet filament in E-type tips. Our most accurate estimates are in the range of 0.3–0.6 μ, that is, 3–4 gold sections (Figs. 11 and 12) from 9D + 2 through 8 (S, D) + 2 to all singlet patterns. In longitudinal sections of tips, discrepancies of filament length are also apparent but are more difficult to estimate accurately. If we assume that all displacement (Δl) of the filaments at the tip is due to discrepancies of arc length (distal vs. proximal filament) in the circular portions

FIGURE 11. Evidence for sliding filaments. *a*. Adjacent serial sections from frontally pointing lateral cilia: E-type tips. Bridge (arrow) at top of cross-section; arms clockwise. Apparent termination order of filaments [from Satir (14)]: long to short (2,3), 1, 4, 9, 5, 8, 6, 7. In one section thickness, two filaments of 9D + 2 pattern become singlets; in another section thickness (not shown), a 9 (S,D) pattern with two singlets becomes 9 (S,D) with four singlets; in a third section thickness, the original short-appearing filaments drop out of the tip; in a fourth section thickness (not shown), the tip simplifies to an all singlet pattern. This allows calculation of Δl. *b*. Adjacent serial sections from abfrontally pointing lateral cilia: E-type tips. Bridge (arrow) at bottom; arms counterclockwise. Apparent termination order of filaments [from Satir (14)]: long to short (5,4), 3, 6, 7, 2, 8, 1, 9. × 96,000 (*a*); × 106,000 (*b*).

of the bent cilium, then

$$\Delta l = \frac{2\pi d\alpha}{360} = 0.0035\alpha \qquad (4)$$

where d is the diameter of the axoneme. Thus $\Delta l/\alpha$ is a constant dependent only on the axonemal diameter (0.2 μ), a parameter that is exceedingly stable in cilia and flagella of most organisms. The Δl values obtained from serial sections are in general agreement with the values predicted from measurements of α; if anything, the former are too large. The displacement of filaments per degree of ciliary bend is 35 A, reasonably small.

DISCUSSION

Support for a Sliding Filament Mechanism

Additional support for a mechanism of ciliary motility involving sliding peripheral filaments comes from several studies. Horridge (15) has examined the ctenophore *Beroë*, where all axonemes in a single comb macrocilium are bounded by a single membrane. In different stroke stages within the comb, buckling or diameter changes of certain axonemes on the concave side of the macrocilium should be apparent if filament contraction occurred. This is not observed. An active sliding mechanism between filaments 2–4 vs. 6–8 is postulated to account for the motion. Brokaw (16) has observed that, in thiourea-inhibited sea urchin spermatozoa, wave patterns are obtained where part of the flagellum is inhibited, but a more proximal part is still active. In these cases the head of the spermatozoon maintains a constant orientation with respect to the inhibited distal zone. This could be accounted for by the presence in the axoneme of inextensible filaments which are bound together in the basal region and in the inhibited zone, but are free to slide in the active region. Phillips (17) has described changes in spiraling of a complex array of filaments in *Sciara* sperm, similar in morphology to the axonemal doublets of normal cilia, that could be accounted for if the filaments slid past one another during morphogenesis. Finally, several years ago Afzelius (18) noted the common occurrence of two types of tips in sea urchin spermatozoa, (9S + 2 and S,D arrays) that are compatible with the model proposed above.

Unit of Activity

The ciliary beat is generally thought to be initiated at the level of the basal body, perhaps at certain filaments. Our present model suggests that, as bending begins, peripheral filaments on one side of the cilium slide with respect to those on the opposite side. Bending is initially confined to the base of the cilium. It is possible to consider that equations 1 and 2 define a shaft length (U) measured along the central pair which is the unit that bends (Figs. 13–15).

Within this unit, Δl increases as the molecular events coupled with sliding proceed. Since the filaments are fixed at the base, the shear generated causes the unit to be bent into an arc. The radius of curvature of the arc decreases

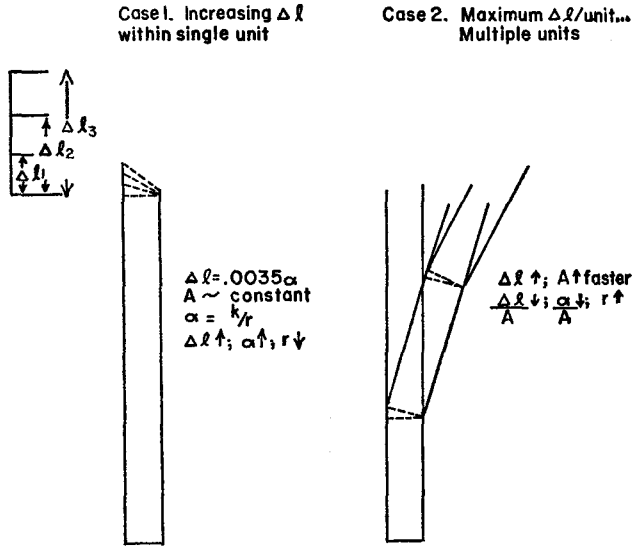

FIGURE 13. Method for determining unit length U. Δl increases as the cilium bends. As long as bending is confined to one unit (U), r decreases (case 1). When more than one unit begins to act (case 2), A increases faster than Δl, $\Delta l/A$ decreases, and r rises; a minimal r then corresponds to the maximum Δl in a single unit.

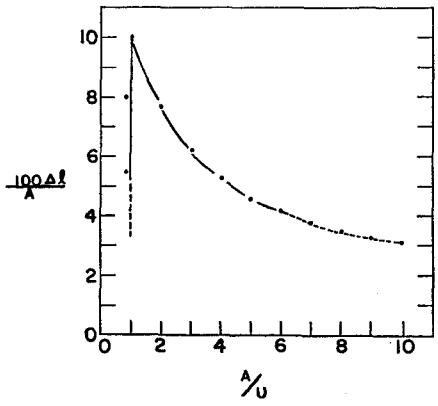

FIGURE 14. $\Delta l/A$ as a function of the number of units active. The unbroken lines represent the range of measurements from Fig. 4.

as Δl, and hence α, increase. It is not unlikely that, by analogy to muscle, sliding occurs in quantum steps. A maximum distortion of the unit is reached when an additional sliding step is no longer sufficient to overcome the resistance of the unit to further bending. At this time, the second unit is fired, and A rises rapidly as Δl increases further. The maximum distortion of the most

basal unit under these conditions corresponds to a minimal radius of curvature, which is easily calculated from the equations. This occurs ar $r = 1.97\ \mu$ and $\alpha = 51°$, which is equivalent to Δl of about $0.179\ \mu$ and $A = 1.78\ \mu = U$ (Table III). It seems reasonable to suggest that one quantal displacement

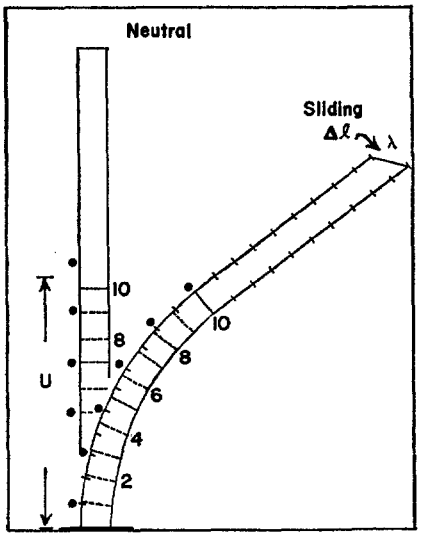

FIGURE 15. Proposed model for bending accompanied by sliding. Drawn to scale (full length of axoneme not shown). Dashed lines are cross-sectional cuts of axoneme. In bent cilium these are $U/10\ \mu$ apart at their midpoints. Note the displacement of these lines with respect to the indicated sites on the outer filament in vernier fashion. Successive displacements differ by approximately the length of one 14S dynein molecule.

TABLE III

GEOMETRY OF THE CILIUM WHEN $\alpha = 51°$; r MINIMAL

	r	A
	μ	μ
cp	1.97	1.78*
pf_o	2.07	1.85
pf_i	1.87	1.67
	$d = 0.2$	$\Delta l = 0.18$‡

Abbreviations: cp = measurements to or along central pair; pf_o = measurements to or along outermost peripheral; pf_i = measurements to or along innermost peripheral.

* U.

‡ Measured arm-to-arm distance: 175 A $\sim$ 1. 14S dynein. $\Delta l \sim 10$. 14S dynein = (30S dynein?).

generated by sliding would be about $0.0175\ \mu$ (measured periodicity of arms), or roughly one 14S dynein molecule. One can then estimate the maximum number of quantal displacements within a unit, U; i.e. $\sim$10. The correspondence between Δl within a unit and the length of one 30S dynein may be purely coincidental, or the coupling of 14S dynein molecules may favor this length, the sites on the filaments at opposite sides of each length $U/10$ capable of being successively displaced in vernier fashion by one more 14S dynein

than their nearest basal neighbors (Fig. 15). This suggestion is, of course, highly speculative, but would fit the empirical data.

At present, it does not seem possible to choose between two alternative interactions that might account for sliding: between arms and matrix protein, or between subfiber *a* of one peripheral doublet and subfiber *b* of its neighbor. A preliminary report by Renaud, Rowe, and Gibbons (19) suggests that an actin-like protein is localized in the doublet wall. The matrix, on the other hand, sometimes contains well-organized elements, such as periodic spokes or thin filaments, that are attractive morphological counterparts to the arms. The central pair is often asymmetrically positioned at the tip region. When this is so, it is found nearest the shorter-appearing filaments. Upon bending an elastic rod fixed at its basal end, cross-section changes will be introduced corresponding to the stretch of the outer region and the compression of the inner region. In the cilium, the matrix would be correspondingly stretched or compressed as sliding occurs when the apparent position of the central pair is altered.

Sliding and Wave Propagation

Although the generation of bending at the base of the cilium is coupled to displacement at the tip, one requirement of equation 4 is that, as the bending wave moves up the shaft, no further displacement occur (α constant) until the restoration of the original condition, when the wave reaches the cilium tip. Thus, unbending of the basal unit must be accompanied by corresponding bending of a subsequent unit. The analysis of bend propagation by Brokaw (4, 12) seems applicable to this part of the motility mechanism, which probably depends on the elastic properties of the ciliary shaft. The actual mode of bend transmission from element to element along the shaft may be still more complicated, since the S shape of flagellar and sometimes of ciliary waves requires the preservation or generation of two antagonistic bends and the straight region between them.

This work was supported by a grant from the U.S. Public Health Service (GM-09732).

REFERENCES

1. FAWCETT, D. W. 1962. *In* The Cell. J. Brachet and A. E. Mirsky, editors. Academic Press, Inc., New York. **2**:217.
2. SATIR, P. 1965. *Protoplasmalogia.* **IIIE.**
3. SLEIGH, M. A. 1962. The Biology of Cilia and Flagella. Pergamon Press, Oxford.
4. BROKAW, C. J. 1966. *J. Exptl. Biol.* **45**:113.
5. GIBBONS, I. R. 1965. *Arch. Biol. (Liege).* **76**:317.
6. GIBBONS, I. R. 1967. *In* Molecular Organization and Biological Function. J. M. Allen, editor. Harper and Row, New York. 211.

7. GRIMSTONE, A. V., and A. KLUG. 1966. *J. Cell Sci.* **1**:351.
8. GIBBONS, I. R., and A. J. ROWE. 1965. *Science.* **149**:424.
9. GRAY, J. 1930. *Proc. Roy. Soc.* (*London*), *Ser. B.* **107**:313.
10. SATIR, P. 1963. *J. Cell Biol.* **18**:345.
11. SATIR, P. 1961. Thesis. The Rockefeller University, New York.
12. BROKAW, C. J. 1965. *J. Exptl. Biol.* **43**:155.
13. BROKAW, C. J., and L. WRIGHT. 1963. *Science.* **142**:1169.
14. SATIR, P. 1965. *J. Cell Biol.* **26**:805.
15. HORRIDGE, G. A. 1965. *Proc. Roy. Soc.* (*London*), *Ser. B.* **162**:351.
16. BROKAW, C. J. 1966. *Am. Rev. Respirat. Diseases.* **93**(Pt. 2):32.
17. PHILLIPS, D. M. 1966. *J. Cell Biol.* **30**:499.
18. AFZELIUS, B. 1959. *J. Biophys. Biochem. Cytol.* **5**:269.
19. RENAUD, F. L., A. J. ROWE, and I. R. GIBBONS. 1966. *J. Cell Biol.* **31**:92A. (Abstr.)

NOTE A Discussion of the Session on Contractile Processes in Nonmuscular Systems begins on page 288.